J. Fluid Mech. (1996), vol. 325, pp. 261–282

The growth of periodic waves in gas-fluidized beds

By S. E. HARRIS

Mathematical Institute, University of Oxford, 24-29 St. Giles', Oxford OX1 3LB, UK

(Received 16 August 1995 and in revised form 3 April 1996)

In this paper, we analyse the development of initially small, periodic, voidage disturbances in gas-fluidized beds. The one-dimensional model was proposed by Needham & Merkin (1983), and Crighton (1991) showed that weakly nonlinear waves satisfied a perturbed Korteweg–de Vries or KdV equation. Here, we take periodic cnoidal wave solutions of the KdV equation and follow their evolution when the perturbation terms are amplifying. Initially, all such waves grow, but at a later stage a rescaling shows that shorter wavelengths are stabilized in a weakly nonlinear state. Longer wavelengths continue to develop and eventually strongly nonlinear solutions are required. Necessary conditions for periodic waves are found and matching back onto the growing cnoidal waves is possible. It is shown further that these fully nonlinear waves also reach an equilibrium state. A comparison with numerical results from Needham & Merkin (1986) and Anderson, Sundaresan & Jackson (1995) is then carried out.

1. Introduction

Fluidized beds are two-phase flow systems used in industry when a large contact surface area between solid particles and a fluid is required. The particles are typically between 50μm and 1 mm in diameter and lie in a deep layer on a porous plate. Fluid is then forced upward through the system with a high enough velocity so that the drag on the particles balances gravity. This results in the particles becoming mobile and buoyant and the fluidized bed exhibits liquid-like phenomena. Increasing the fluid velocity beyond the critical value needed for fluidization leads to the expansion of the bed. This is relatively uniform for most liquid-fluidized beds and for gas-fluidized beds with very fine particles, although wavy structures exist, indicating the presence of instabilities. At higher velocities still, this regime breaks down and gas-fluidized beds bubble and resemble a boiling liquid. In very narrow tubes, the bubbling cannot occur and instead we have slugging, with alternating horizontal bands of particle-rich and depleted regions. These propagate vertically upward by particle raining at the interfaces.

The model used here is one-dimensional, which is appropriate for the study of fluidization in narrow tubes, and was suggested by Needham & Merkin (1983) with a modification proposed by Harris & Crighton (1994). Many similar models are present in the literature, for instance see Jackson (1963*a*, *b*), Garg & Pritchett (1975), Homsy, El-Kaissy & Didwania (1980), Foscolo & Gibilaro (1984, 1987). They use the concept of interacting continua so that the point variables are averaged over volumes which are large compared to particle size and spacing, but small compared to the whole

system. This leads to continuum equations for the particles and the fluid which can be treated as two, interpenetrating, one-phase fluids with suitable interaction terms. In addition, we restrict consideration to gas-fluidized beds as this simplifies the system, reducing it to two equations for the particle phase.

In this paper, we examine the temporal development of vertically travelling, one-dimensional periodic wavetrains in gas-fluidized beds. Crighton (1991) looks at the linear stability conditions and then derives a weakly nonlinear equation valid on the unstable side of the threshold. At leading order, this is the Korteweg–de Vries or KdV equation and perturbation terms are amplifying for $O(1)$ wavelengths but balance or dissipate for small wavelengths. Harris & Crighton (1994) examine the amplifying case starting with a KdV soliton as an initial condition. The development is followed through several weakly nonlinear regimes until it evolves into a fully nonlinear $O(1)$ wave which Crighton (1995) refers to as a 'voidon'. Here, we perform a similar analysis, but begin instead with the periodic cnoidal solution of the KdV equation for our initial state. The temporal development of this cnoidal wavetrain is then followed in §3. It is discovered that cnoidal waves of all wavelengths are amplified at first, with the smaller wavelengths growing faster. However, these all have a finite-time singularity in their amplitude and velocity, which is not physically possible. Near this singularity, a rescaling is carried out and it is then found that the shorter wavelengths are stabilized at this weakly nonlinear stage. The finite-time singularity, although weakened, is still present for the longer wavelengths and they continue to grow until they eventually become fully nonlinear.

In §4, we examine the fully nonlinear periodic solutions and find necessary conditions for these to exist. We demonstrate that they match back onto the growing cnoidal waves in the weakly nonlinear state and also that they equilibrate. Thus, the finite-time singularity was an artefact of our weakly nonlinear approximation and there is no actual blow-up.

The case of hindered settling in a dilute suspension is considered briefly in §5. The situation is the same as fluidized beds except for a much higher background voidage and a different reference frame. The results of our analytical study are then compared with numerical computations by Needham & Merkin (1986) and Anderson, Sundaresan & Jackson (1995). The former study relates to quasi-steady, periodic travelling wave solutions of the full equations. The latter paper is a comprehensive investigation following the temporal development of sinusoidal waves into fully developed $O(1)$ solutions for a very similar set of equations. These are found to agree well with the analytical results presented here.

2. Model equations

The model equations represent mass and momentum conservation in the particle phase. It is useful to write them in terms of the averaged vertical particle velocity v and a voidage fraction ϕ (the volume of fluid in unit volume of the two-phase mixture). Theoretically, the voidage can vary between 0 and 1, the pure solid and pure fluid limits, but in practice, there is a larger lower limit on ϕ since there is always residual fluid in the spaces between the particles. The state of uniform fluidization is given by

$$\phi = \phi_0, \qquad v = 0, \qquad u = U_0, \tag{2.1}$$

where the voidage fraction and averaged vertical fluid velocity U_0 are constant and there is zero vertical particle velocity.

We examine the fluidized bed equations in the non-dimensional form

$$-\frac{\partial \phi}{\partial t} + \frac{\partial}{\partial x}([1-\phi]v) = 0, \tag{2.2}$$

$$(1-\phi)\left(\frac{\partial v}{\partial t} + v\frac{\partial v}{\partial x}\right) = \frac{(1-\phi)}{F^2}\left(\frac{\phi_0}{\phi}\right)^{n+1}\left(1-\frac{v}{\phi_0}\right) - \frac{(1-\phi)}{F^2} - p_s'(\phi)\frac{\partial \phi}{\partial x} + \frac{1}{R}\frac{\partial^2 v}{\partial x^2}, \tag{2.3}$$

where $F^2 = {U_0}^2/gh$ is the square of a Froude number and $R = \rho_s U_0 h/\mu_s$ is a particle-phase Reynolds number, with h being a localized, voidage disturbance lengthscale and ρ_s, μ_s being the density and effective viscosity of the particle phase. The index n occurs in the Richardson–Zaki relation, which is an experimental correlation relating the fluid velocity U_0 to the voidage fraction ϕ_0 (Richardson 1971). It is weakly dependent on the Reynolds number of the flow, but here we will assume it is a constant lying in the range 3 to 4. The function $p_s(\phi)$ is a particle pressure and has a stabilizing influence. This was omitted in earlier models such as Jackson (1963*a*) and Murray (1965) but in this case the linear stability analysis predicts the bed to be unstable at all flow rates, which disagrees with experimental observations. Here we set

$$p_s(\phi) = P_s\frac{(1-\phi)}{(\phi-\phi_{cp})}, \tag{2.4}$$

so that the particle pressure vanishes in the pure fluid limit when $\phi = 1$ and becomes infinite at close packing at $\phi = \phi_{cp}$ when no more fluid can be removed without crushing the particles. This is the modification made to Needham & Merkin's (1983) model by Harris & Crighton (1994) so that a weakly unstable flow regime could be reached by increasing the flow velocity through the stable state. Provided this criterion holds, however, the exact form of $p_s(\phi)$ is not very important as it is only the sign of the first two derivatives of the function evaluated at the uniform voidage fraction which have an effect on the analysis. For a detailed description of the derivation of these equations see Harris & Crighton (1994).

Experimental results suggest that the Froude number is small and so in later calculations, we use the assumption in Needham & Merkin (1983) that

$$F \ll 1, \tag{2.5}$$

and treat this as our perturbation parameter in looking at small disturbances from the uniform state. A linear stability analysis following Needham & Merkin (1983) and Crighton (1991) then yields

$$\phi_\tau' + \gamma_0\phi_{XXX}' + (\alpha_0^2 - P_0)\phi_0\phi_{XX}' - 2F^2\phi_0\alpha_0\phi_{\tau X}' - F^2\frac{\gamma_0}{\alpha_0}\phi_{\tau XX}' + F^4\phi_0\phi_{\tau\tau}' = 0, \tag{2.6}$$

where ϕ' is the voidage perturbation,

$$X = x - \alpha_0 t, \qquad \alpha_0 = (n+1)(1-\phi_0); \tag{2.7}$$

$$\tau = F^2 t \tag{2.8}$$

is a slow timescale and

$$-p_s'(\phi_0) = P_0 > 0. \tag{2.9}$$

As indicated in Needham & Merkin (1983), if $P_0 > \alpha_0^2$, waves corresponding to all wavenumbers are stable for any F; whereas if $P_0 < \alpha_0^2$, then there is a band of modes

with wavenumbers less than some critical value which are unstable. We are interested in weak instabilities and so we examine the situation

$$\alpha_0^2 - P_0 = F\frac{\delta_0}{\phi_0}, \tag{2.10}$$

where δ_0 is a positive $O(1)$ constant and we now take F to be small. Thus, the first two terms in (2.6) are at leading order, with the others acting as perturbations. For long wavelengths, i.e. $X = O(1)$, the third term dominates those to its right and so we have slow growth. The rescaling $X = O(F^{1/3})$ and $\tau = O(F)$ retains the first two terms at leading order but leads to the third and fifth terms being of the same magnitude at the next order. However, the fifth term does not materially alter the stability characteristics so that we still have growth. At shorter wavelengths still, when $X = O(F^{1/2})$, the fifth term is the leading-order perturbation with the third and fourth terms next. Again, the $\phi'_{\tau XX}$ term does not affect the stability but the ϕ'_{XX} and $\phi'_{\tau X}$ terms balance so the shorter wavelengths do not grow, as discussed in Harris & Crighton (1994). Here, we restrict attention to the growing long wave modes, so we consider X to be $O(1)$.

Eventually a linear approximation ceases to be valid when the wave amplitude becomes too large and we must then consider weakly nonlinear effects. To do this, we rescale the equations using

$$v = F^2 v', \qquad \phi = \phi_0 + F^2\phi', \tag{2.11}$$

as well as (2.7) and (2.8). This leads to the $O(1)$ approximation

$$v' = -(n+1)\phi', \tag{2.12}$$

where ϕ' satisfies

$$\begin{aligned}\phi'_\tau + \beta_0\phi'\phi'_X + \gamma_0\phi'_{XXX} = &-F\delta_0\phi'_{XX}\\ &+F^2\left[2\frac{(n+1)}{\phi_0}\phi'\phi'_\tau + \frac{\gamma_0}{\alpha_0}\phi'_{\tau XX} - \frac{\gamma_0}{(1-\phi_0)}(\phi'^2)_{XXX}\right]\\ &+F^2(n+1)\frac{\gamma_0}{\phi_0}\phi'^2\left(\frac{\phi'_{XX}}{\phi'}\right)_X\\ &-F^2\frac{(n+1)(n+2)}{2\phi_0^2}\left[3\phi_0 - 2n(1-\phi_0)\right]\phi'^2\phi'_X\\ &+F^2\phi_0\alpha_0\left[2\phi'_{\tau X} - (n+1)(\phi'^2)_{XX}\right]\\ &-F^2\phi_0 P_1\left[(\phi'_X)^2 + \phi'\phi'_{XX}\right] + O(F^3),\end{aligned} \tag{2.13}$$

and the $O(1)$ constants β_0, γ_0 and P_1 are given by

$$\beta_0 = -(n+1)\left(2 + n - \frac{n}{\phi_0}\right), \qquad \gamma_0 = (n+1)\frac{\phi_0}{R}, \qquad P_1 = p_s''(\phi_0) > 0. \tag{2.14}$$

Equation (2.13) contains an additional $O(F^2)$ term omitted from Harris & Crighton (1994); however, it has no effect on the analysis there as it vanishes in a secularity integral.

In the context of fluidized beds, experimental results by Leva (1959) show that values of ϕ_0 between 0.4 and 0.5 are suitable for an initially packed bed so that with $n = 3$,

$$\phi_0 < \frac{n}{n+2} \tag{2.15}$$

is satisfied and thus $\beta_0 > 0$. In §5, we briefly examine what happens when $\beta_0 < 0$, which is appropriate for hindered settling of a dilute suspension, but for the moment, we restrict β_0 to be positive.

In (2.13), we have the KdV equation at leading order, with perturbation terms on the right-hand side. The first of these is the negative dissipation term present in the linearized equation (2.6) and it represents amplification. The $O(F^2)$ terms include $\phi'_{\tau X}$ which modulate the growth for short wavelengths.

Here, we are interested in periodic solutions, rather than the solitary wave solutions considered in Harris & Crighton (1994). Therefore, as our initial state, we take the periodic cnoidal wave solutions of the KdV equation given by

$$\phi' = \lambda + \frac{12\gamma_0}{\beta_0} m\kappa^2 \mathrm{cn}^2 \kappa\eta, \tag{2.16}$$

where

$$\eta = X - x_0 - [4\gamma_0\kappa^2(2m-1) + \beta_0\lambda]\tau \tag{2.17}$$

is a travelling wave coordinate, λ, κ and x_0 are arbitrary constants, cn is the Jacobian elliptic function (Abramowitz & Stegun 1964) and m is the parameter of cn which, without loss of generality, we take to satisfy $0 \leqslant m \leqslant 1$.

For a description of the Jacobian elliptic functions in relation to periodic solutions of the KdV equation, see Drazin & Johnson (1989). Here, we note that as

$$m \to 0, \qquad \mathrm{cn}(\theta|m) \to \cos\theta, \tag{2.18}$$

so this gives a linear wave approximation. As

$$m \to 1, \qquad \mathrm{cn}(\theta|m) \to \operatorname{sech}\theta, \tag{2.19}$$

thus the solution (2.16) tends to the single soliton solution of the KdV equation and this is the most nonlinear limit. The amplitude, velocity and wavelength of the cnoidal solution all depend on m in different ways. Abramowitz & Stegun (1964) define the quarter-period of $\mathrm{cn}(\theta|m)$ as $K(m)$, so that $K(0) = \pi/2$ and $K(1) = \infty$ as the soliton solution can be thought of as having an infinite wavelength. It can be shown that $K(m)$ is a monotonic increasing function of m and we also note that $\mathrm{cn}^2(\theta|m)$ actually has a period $2K(m)$ (and not $4K(m)$).

Because of the complicated nature of the m dependence, we choose to keep m constant in the analysis which follows. We are interested in disturbances to the uniform state $\phi = \phi_0$ and we want this to remain a solution of the equations. Therefore, we fix λ by insisting that the perturbation ϕ' has zero mean displacement over one wavelength. Thus, we must have

$$\lambda = -\frac{6\gamma_0}{\beta_0}\frac{m\kappa^2}{K}\int_{-K}^{K} \mathrm{cn}^2\theta \, \mathrm{d}\theta. \tag{2.20}$$

This leaves us with the two constants κ and x_0 and in the next section, we allow them to be slowly varying so that we have growing cnoidal waves.

3. Perturbed Korteweg–de Vries equation

In this section, we examine the effects on cnoidal waves of including the perturbation terms on the right-hand side of equation (2.13). The analysis closely parallels the corresponding section in Harris & Crighton (1994), but is given in detail here in order that the material is understandable without constant reference to the earlier paper.

We now look for an asymptotic expansion for ϕ' in powers of F in the form

$$\phi' = \phi_1(X, \tau, T) + F\phi_2(X, \tau, T) + O(F^2),$$

where a slower timescale

$$T = F\tau, \tag{3.1}$$

is introduced to eliminate higher-order secular terms (Leibovich & Seebass 1974; Nayfeh 1973). The leading-order solution, ϕ_1, is given by the cnoidal wave in (2.16), but with κ and x_0 now allowed to vary on this long timescale T. This permits the possibility of growing solutions and also a phase shift (although this is unimportant). The introduction of the timescale T also adds an extra term $-F\phi'_T$ onto the right-hand side of equation (2.13).

The second-order solution ϕ_2 satisfies

$$\mathscr{L}\phi_2 \equiv -c_1\phi_{2\eta} + \beta_0(\phi_1\phi_2)_\eta + \gamma_0\phi_{2\eta\eta\eta} = -\delta_0\phi_{1\eta\eta} - \phi_{1T}. \tag{3.2}$$

The condition for ϕ_2 to exist is given by

$$\int_{-K}^{K} \frac{1}{\kappa}\phi_1\phi_{1T}\,\mathrm{d}\theta = -\int_{-K}^{K} \delta_0\kappa\phi_1\phi_{1\theta\theta}\,\mathrm{d}\theta \tag{3.3}$$

(see Courant & Hilbert 1962) where $\theta = \kappa\eta$. This is an integral formulation of the necessary secularity condition. We can now substitute in for ϕ_1 using (2.16) remembering that m is fixed, but κ and hence λ from (2.20) depend on T. Using the result from Appendix A,

$$\int_{-K}^{K} \mathrm{cn}^2\theta[5m\mathrm{cn}^4\theta + 4(1-2m)\mathrm{cn}^2\theta + 3(m-1)]\,\mathrm{d}\theta = 0, \tag{3.4}$$

to eliminate integrals in $\mathrm{cn}^6\theta$, we can simplify (3.3) to give

$$\kappa_T = b(m)\kappa^3, \tag{3.5}$$

where

$$f(m) = 3\int_{-K}^{K} \mathrm{cn}^4\theta\,\mathrm{d}\theta - \frac{1}{K}\left[\int_{-K}^{K} \mathrm{cn}^2\theta\,\mathrm{d}\theta\right]^2, \tag{3.6}$$

$$g(m) = 2(1-m)\int_{-K}^{K} \mathrm{cn}^2\theta\,\mathrm{d}\theta + (2m-1)\int_{-K}^{K} \mathrm{cn}^4\theta\,\mathrm{d}\theta, \tag{3.7}$$

$$b(m) = \frac{8}{5}\frac{g(m)}{f(m)}\delta_0. \tag{3.8}$$

If we set $m = 1$, so that $K = \infty$ and $\mathrm{cn}\theta = \mathrm{sech}\,\theta$, we obtain

$$\kappa_T = \tfrac{8}{15}\delta_0\kappa^3,$$

which agrees with the result obtained in the perturbed soliton theory in Harris & Crighton (1994). If $m = 0$, then $K = \pi/2$, $\mathrm{cn}\theta = \cos\theta$ and $b = 8\delta_0/5$. Thus the amplification rate is greater for $m = 0$ than for $m = 1$. In fact, b is a monotonic decreasing function of m but is positive for $0 \leqslant m \leqslant 1$ (see figure 1). Thus all the periodic waves are amplified and those with shorter wavelengths are amplified faster.

If we integrate equation (3.5) and set $\kappa(0) = 1$, then we obtain

$$\kappa(T) = \left(\frac{T_0}{T_0 - T}\right)^{1/2}, \tag{3.9}$$

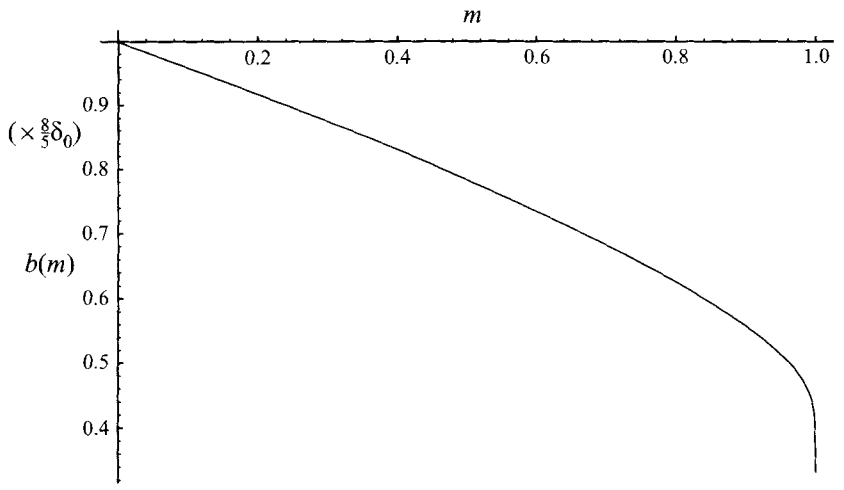

FIGURE 1. A graph of the growth rate coefficient $b(m)$.

where

$$T_0 = \frac{1}{2b(m)}. \tag{3.10}$$

Thus we have a finite-time singularity at $T = T_0$ which causes the solution for ϕ' to blow up, which is physically unacceptable. Another effect is to shorten the wavelength which is proportional to $1/\kappa(T)$. To see the changes this causes, we must return to the full set of equations and rescale the variables near the finite-time singularity using

$$\left.\begin{aligned} -F^{2a}\hat{T} = T_0 - T, \quad \hat{x} = F^{-a}(X - x_0 - \xi), \\ \hat{\kappa}(\hat{T}) = F^a\kappa(T), \quad \frac{\partial\xi}{\partial\tau} = F^{-2a}\hat{c}_1, \\ \hat{c}_1 = 4\gamma_0(2m-1)\hat{\kappa}^2(\hat{T}) + \beta_0\hat{\lambda}, \quad \phi = \phi_0 + F^{2-2a}\phi', \qquad v = F^{2-2a}v', \end{aligned}\right\} \tag{3.11}$$

where $\hat{T}$, $\hat{x}$, $\hat{\kappa}$, $\hat{c}_1$, $\hat{\lambda}$, ϕ' and v' are $O(1)$ quantities, with $\hat{\lambda}$ being the same as λ but with $\hat{\kappa}$ replacing κ. Substituting these back into (2.2) and (2.3) gives

$$\begin{aligned} &-\hat{c}_1\phi'_{\hat{x}} + \beta_0\phi'\phi'_{\hat{x}} + \gamma_0\phi'_{\hat{x}\hat{x}\hat{x}} = -F^{1+a}\left[\phi'_{\hat{T}} + \delta_0\phi'_{\hat{x}\hat{x}}\right] \\ &-F^{2-2a}\left[2\hat{c}_1\frac{(n+1)}{\phi_0}\phi'\phi'_{\hat{x}} + \frac{\gamma_0\hat{c}_1}{\alpha_0}\phi'_{\hat{x}\hat{x}\hat{x}} + \frac{\gamma_0}{(1-\phi_0)}(\phi'^2)_{\hat{x}\hat{x}\hat{x}} - (n+1)\frac{\gamma_0}{\phi_0}\phi'^2\left(\frac{\phi'_{\hat{x}\hat{x}}}{\phi'}\right)_{\hat{x}}\right] \\ &-F^{2-2a}\frac{(n+1)(n+2)}{2\phi_0^2}\left[3\phi_0 - 2n(1-\phi_0)\right]\phi'^2\phi'_{\hat{x}} \\ &-F^{2-a}\phi_0\alpha_0\left[2c_1\phi'_{\hat{x}\hat{x}} + (n+1)(\phi'^2)_{\hat{x}\hat{x}}\right] \\ &-F^{2-a}\phi_0 P_1\left[(\phi'_{\hat{x}})^2 + \phi'\phi'_{\hat{x}\hat{x}}\right] + o(F^{1+a}, F^{2-a}). \end{aligned} \tag{3.12}$$

Our previous analysis corresponded to $a = 0$, but we must now consider the regime $0 < a < 1$ and allow the perturbation expansion for ϕ' to contain non-integral powers of F. For $a < 1/3$, the $O(F^{1+a})$ terms form the leading-order perturbations and these are precisely the same terms that we retained previously. Thus the amplitude growth rate is still given by equation (3.5), although in rescaled coordinates. When $a = 1/3$, the $O(F^{2-2a})$ terms become the same size as those of $O(F^{1+a})$. This is equivalent to the rescaling on the linear equation (2.6) needed to make the ϕ'_{XX} and $\phi'_{\tau XX}$ terms of the same order. In the linear situation, the $\phi'_{\tau XX}$ had no significant effect on the

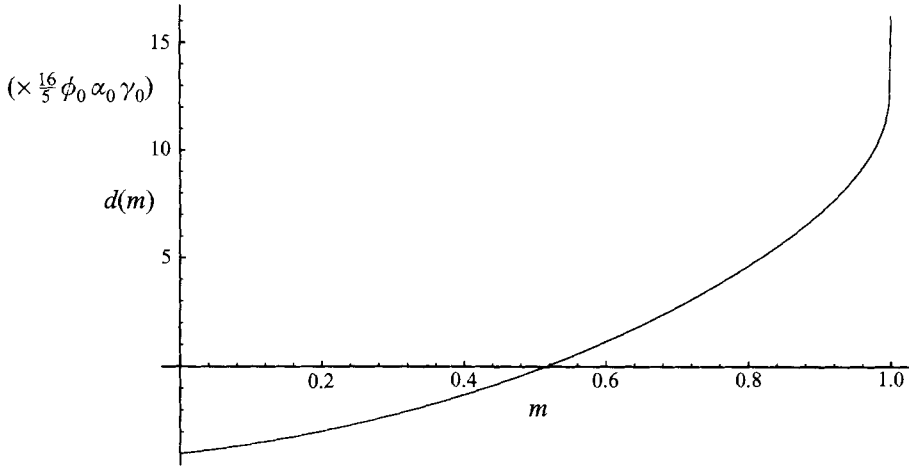

FIGURE 2. A plot of $d(m)$ for typical parameter values.

stability (merely altering the size of some of the coefficients) and the same holds true in the weakly nonlinear situation. Thus a change in secularity condition does not occur as the $O(F^{2-2a})$ terms vanish in the compatibility integral (as also happened in the soliton case examined in Harris & Crighton 1994). For $1/3 < a < 1/2$, the asymptotic sequence for ϕ' is simply reordered, with the $O(F^{1+a})$ and $O(F^{2-2a})$ terms swopping over and there is no fundamental change in the solution. When $a = 1/2$, the $O(F^{1+a})$ and $O(F^{2-a})$ terms become of the same order (equivalent to the ϕ'_{XX} and $\phi'_{\tau X}$ being the same order in the linear equation). Now there is a change in the secularity condition to

$$\hat{\kappa}_{\hat{T}} = b(m)\hat{\kappa}^3 + d(m)\hat{\kappa}^5, \tag{3.13}$$

where

$$\begin{aligned} d(m) = {} & \frac{16}{5}\phi_0\alpha_0\gamma_0\frac{g(m)}{f(m)}\left\{4(2m-1) - \frac{6m}{K}\int_{-K}^{K}\mathrm{cn}^2\theta\,\mathrm{d}\theta\right\} \\ & + \frac{96}{35}\frac{1}{f(m)}\frac{\gamma_0}{\beta_0}\phi_0[P_1 + 2\alpha_0(n+1)]\left\{2[2(2m-1)^2 + 5(1-m)m]\int_{-K}^{K}\mathrm{cn}^4\theta\,\mathrm{d}\theta\right. \\ & \left. + \left[3(1-m)(2m-1) - \frac{7m}{2K}g(m)\right]\int_{-K}^{K}\mathrm{cn}^2\theta\,\mathrm{d}\theta\right\}, \end{aligned} \tag{3.14}$$

and $b(m)$, $g(m)$, $f(m)$ are unchanged from (3.6)–(3.8).

The function d is monotonic increasing in m, but is negative for small m and positive for large m. Using suitable values for ϕ_0, n and P_1 etc., figure 2 shows that the change from negative to positive values occurs at $m = m_1$, with $m_1 \approx 1/2$. When $d < 0$, the waves equilibrate at this weakly nonlinear stage as the two terms on the right-hand side of (3.13) can balance each other. So, although the shorter wavelengths were initially faster growing, they stabilize at this amplitude. However, for $m > m_1$, the wave continues to grow and we eventually expect the $\hat{\kappa}^5$ terms to dominate those of $\hat{\kappa}^3$. Thus with another rescaling, we have

$$\hat{\kappa}_{T'} = d(m)\hat{\kappa}^5. \tag{3.15}$$

Figure 3(*a–c*) shows the amplitude of the wave $A = 12\gamma_0 m\kappa^2/\beta_0$ as a function of time for $m = 0.2$, 0.5 and 0.8 respectively. The first two of these demonstrate that the wave

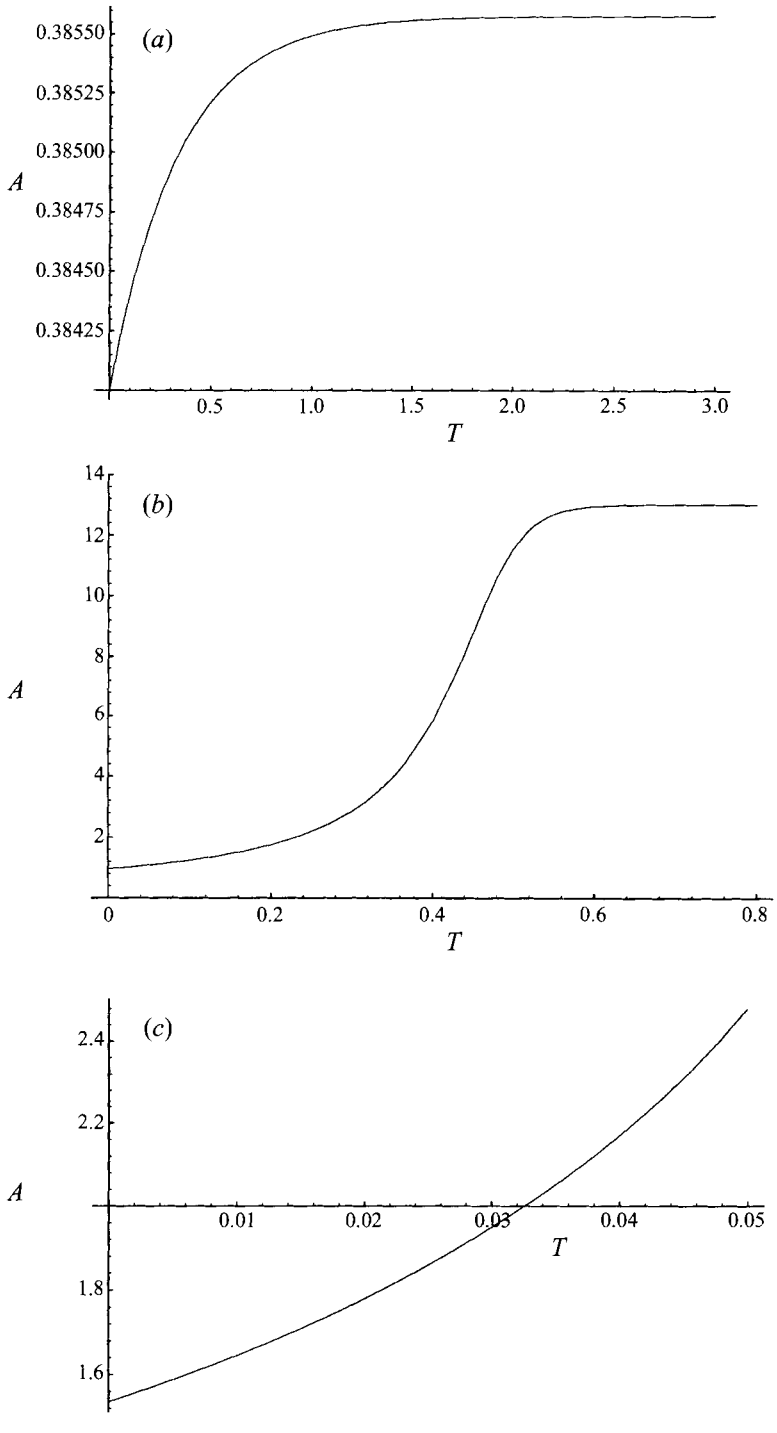

FIGURE 3. Graphs of the amplitude of the periodic waves against time for different values of m: (*a*) $m = 0.2$, (*b*) $m = 0.5$, (*c*) $m = 0.8$.

amplitude equilibrates, whereas the third is in the regime $m > m_1$ and shows that the amplitude increases beyond the point where the weakly nonlinear approximations appply. In this case, a numerical integration of the full equations is required. We suggest that there are no further alterations in the secularity condition whilst the waves remain weakly nonlinear. Eventually, they become fully nonlinear when $a = 1$ and further investigation is then needed to examine the structure and growth of the solution.

4. Finite-amplitude periodic waves

In this section, we find necessary conditions for fully nonlinear periodic solutions to exist. We then show that under these parameter restrictions, the waves can be matched back onto the growing cnoidal solutions found in the previous section. This justifies our claim that we have found all the matching regions and can follow the development of small perturbations through to fully nonlinear disturbances. We also prove that the finite-time singularity in the velocity and amplitude found at the weakly nonlinear stage is, in fact, spurious and that the fully nonlinear waves tend to an equilibrium state. The analysis again follows that for the soliton case in Harris & Crighton (1994).

Upon suitable rescaling for fully nonlinear $O(1)$ disturbances with $\phi = \hat{\phi}$, $v = \hat{v}$ and ζ a travelling wave coordinate, the original system (2.2) and (2.3) becomes

$$c\hat{\phi}_\zeta + [(1-\hat{\phi})\hat{v}]_\zeta = 0, \tag{4.1}$$

$$(1-\hat{\phi})\left(\frac{\phi_0}{\hat{\phi}}\right)^{n+1}\left(1-\frac{\hat{v}}{\phi_0}\right) - (1-\hat{\phi}) + \frac{1}{R}\hat{v}_{\zeta\zeta} = F\left[(1-\hat{\phi})(\hat{v}-c)\hat{v}_\zeta + p_s'(\hat{\phi})\hat{\phi}_\zeta\right], \tag{4.2}$$

where c is an undetermined velocity and the neglected terms are $O(F^2)$. Substituting in perturbation expansions for $\hat{\phi}$, $\hat{v}$,

$$\hat{\phi} = \hat{\phi}_0 + F\hat{\phi}_1 + \cdots, \qquad \hat{v} = \hat{v}_0 + F\hat{v}_1 + \cdots, \tag{4.3}$$

and integrating (4.1) gives

$$\hat{v}_0 = -c\frac{(\hat{\phi}_0 - \phi_0)}{(1-\hat{\phi}_0)}, \tag{4.4}$$

as the uniform state, $\hat{\phi}_0 = \phi_0$ and $\hat{v}_0 = 0$, is a solution of the equations. This expression for $\hat{v}_0$ can be used to eliminate the particle velocity from the momentum equation to yield an equation for the leading-order voidage term $\hat{\phi}_0$. Temporarily dropping the zero subscripts on $\hat{\phi}$ and integrating once gives

$$\frac{c(1-\phi_0)}{2R}\frac{\hat{\phi}_\zeta^{\,2}}{(1-\hat{\phi})^4} = h(\hat{\phi}), \tag{4.5}$$

where

$$h(\hat{\phi}) = \ln\left(\frac{1-\hat{\phi}}{1-\phi_l}\right) + \phi_0^n\int_{\phi_l}^{\hat{\phi}}\left[\frac{(\phi_0 - c)}{z^{n+1}(1-z)} + \frac{c(1-\phi_0)}{z^{n+1}(1-z)^2}\right]\mathrm{d}z, \tag{4.6}$$

and the lower limit ϕ_l of the integration is chosen to be a zero of $\hat{\phi}_\zeta^2$. (This differs from the lower limit of ϕ_0 for solitons.)

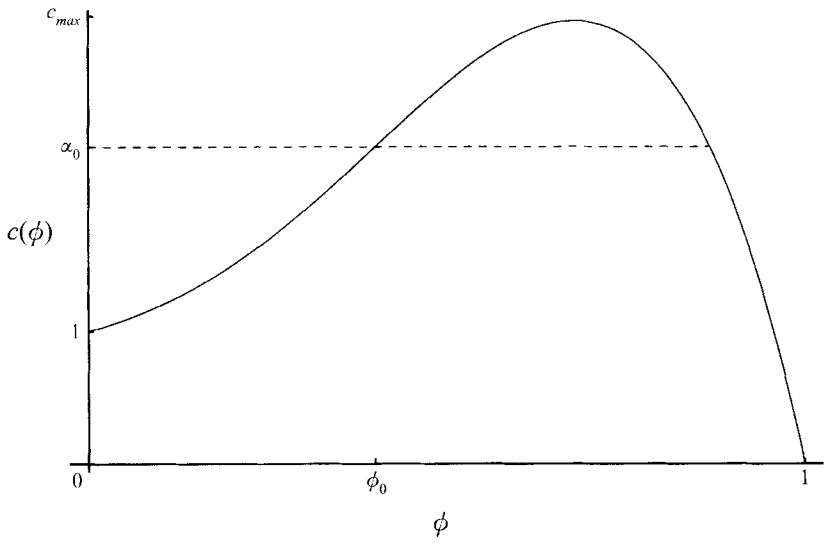

FIGURE 4. A graph of $c(\phi)$ for $h'(\phi) = 0$, $\phi_0 = 0.4$, $n = 3$.

If we set

$$\hat{\phi}_\zeta^{\,2} = f(\hat{\phi}), \tag{4.7}$$

then periodic solutions occur when $\hat{\phi}_\zeta^{\,2}$ is positive between two simple zeros of $f(\hat{\phi})$ (see Drazin & Johnson 1989). Here, we can just examine the zeros of $h(\hat{\phi})$ as the effect of the $(1-\hat{\phi})^4$ term in (4.5) merely serves to modify the shape of the graph without affecting the qualitative solution. (We must necessarily exclude the case $\hat{\phi} = 1$, which corresponds to pure fluid, in order for equation (4.5) to be valid.)

Considering $h'(\hat{\phi})$, we see that $h'(\phi_0) = 0$ and to find the other turning points of h, we rearrange $h'(\hat{\phi}) = 0$ as an equation for the wave velocity c, so

$$c = \phi_0 \frac{(1-\hat{\phi})}{(\hat{\phi}-\phi_0)} \left[\left(\frac{\hat{\phi}}{\phi_0} \right)^{n+1} - 1 \right]. \tag{4.8}$$

This function has a single maximum at $\hat{\phi} = \phi_c$, where

$$\frac{n}{n+2} < \phi_c < 1, \tag{4.9}$$

provided

$$\frac{n}{n+2} > \phi_0. \tag{4.10}$$

Equation (4.10) is identical to the condition $\beta_0 > 0$ and is realistic in the context of fluidized beds. A graph of c as a function of $\hat{\phi}$ for $h'(\hat{\phi}) = 0$ is given in figure 4. The relation (4.8) and figure 4 have already been seen in Göz (1993) where oblique travelling wave solutions in gas- and liquid-fluidized beds have been examined. It can be seen that if

$$c > c_{max},$$

there are no other turning points of $h(\hat{\phi})$; if

$$\alpha_0 < c < c_{max},$$

there are two turning points of h to the right of ϕ_0; and if

$$\alpha_0 > c > 1, \tag{4.11}$$

there is one turning point on each side of ϕ_0. For (4.11) to be possible we need $\alpha_0 = (n+1)(1-\phi_0) > 1$, but this is automatically satisfied when $\beta_0 > 0$. In the case

$$\alpha_0 > 1 > c > 0, \tag{4.12}$$

we have a single turning point to the right of ϕ_0 and lastly, for $c < 0$, there are again no other turning points apart from at $\hat{\phi} = \phi_0$.

We note that

$$h''(\phi_0) = \frac{1}{\phi_0(1-\phi_0)^2}(c - \alpha_0), \tag{4.13}$$

so that $h''(\phi_0)$ is positive if $c > \alpha_0$ and negative if $c < \alpha_0$, giving us minimum and maximum turning points of h respectively. We also observe that

$$h'(\hat{\phi}) \to \left(\frac{\phi_0}{\hat{\phi}}\right)^{n+1}(1-c) \qquad \text{as} \qquad \hat{\phi} \to 0, \tag{4.14}$$

$$h'(\hat{\phi}) \to c\phi_0^n \frac{(1-\phi_0)}{(1-\hat{\phi})^2} \qquad \text{as} \qquad \hat{\phi} \to 1. \tag{4.15}$$

Thus possible graphs for $h(\hat{\phi})$ for the different ranges of the parameter c are shown in figure 5(*a–e*).

We need $h(\hat{\phi})$ to be positive between two simple zeros around ϕ_0 if $c > 0$ and negative if $c < 0$ (from (4.5)) for periodic solutions about the uniform state. Then it is clear that necessary conditions for this are

$$\alpha_0 > c > 0. \tag{4.16}$$

We also require certain other conditions to be satisfied, namely $h(\phi_0) > 0$ and $h(\phi_j) < 0$ for the turning points ϕ_j on either side of ϕ_0. We set ϕ_l, ϕ_u to be the nearest zeros of h to ϕ_0 such that

$$\phi_l < \phi_0 < \phi_u,$$

which gives $h(\phi_0) > 0$ in (4.6) as ϕ_l is the lower limit of the integration.

Needham & Merkin (1986) examine the same equations, with slightly different rescalings (and a different particle pressure but using the definition of $P_0 = -p_s'(\phi_0)$ so that this agrees with ours). They use the Hopf-bifurcation theorem to show that necessary and sufficient conditions for a periodic orbit to bifurcate out of the equilibrium point $(\phi_0, 0)$ in the phase plane (i.e. the uniform state) are

$$\alpha_0 > c > 0, \qquad \alpha_0^2 > P_0 > 0. \tag{4.17}$$

These in fact hold without restricting the Froude number to be small. The first of these is identical to (4.16) and the second condition means $\delta_0 > 0$, so that we are on the unstable side of the threshold in the linear and weakly nonlinear regimes. Therefore there is complete agreement with our criteria.

We examine the expansion for c in the form

$$c = \alpha_0 + F^{2-2a}c_1 + \cdots,$$

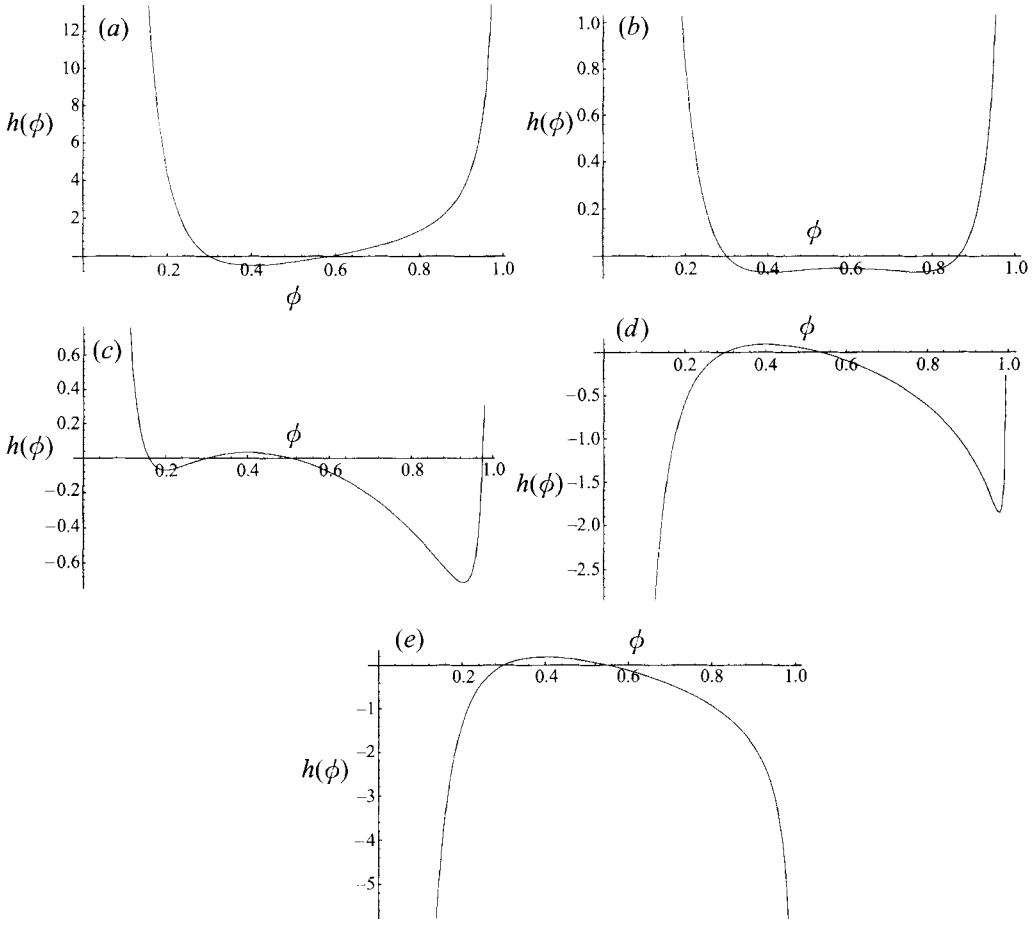

FIGURE 5. Typical graphs of $h(\phi)$ for different values of the velocity c: (*a*) $c > c_{max}$, (*b*) $c_{max} > c > \alpha_0$, (*c*) $\alpha_0 > c > 1$, (*d*) $1 > c > 0$, (*e*) $c < 0$.

which is valid in the weakly nonlinear situation with c_1 given by

$$c_1 = 4\gamma_0(2m-1)\kappa^2 - 6\gamma_0\frac{m\kappa^2}{K}\int_{-K}^{K} \mathrm{cn}^2\theta\,\mathrm{d}\theta, \tag{4.18}$$

from (2.17) and (2.20). Thus in order to satisfy (4.16), we expect to have $c_1 < 0$. A plot of this is given in figure 6, and so we see that c_1 is a monotonic increasing function of m which is negative for most of the range, but is positive close to 1. This suggests that for m close to 1, the weakly nonlinear cnoidal waves are unstable. Thus if the wavelength is too large, we cannot have slowly growing periodic waves and any wavetrains of this sort will break up. Anderson *et al.* (1995) also report indications that for very long waves the periodic behaviour does not persist, but instead becomes time-dependent without settling into any regular pattern. We note that when $c_1 < 0$, the waves travel slower than the linear wave speed α_0, and for fixed m they slow down as they grow.

To match the fully nonlinear periodic solutions back onto the growing cnoidal waves, we first introduce the timescale

$$T - T_0 = F^3 T', \tag{4.19}$$

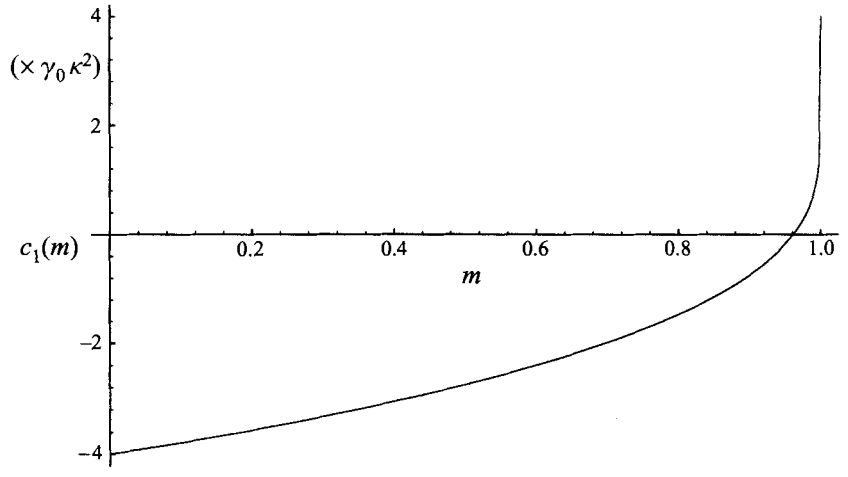

FIGURE 6. The function c_1 plotted against m.

and allow the wave velocity c to change with T'. The effect of this is to add a term $F\hat{\phi}_{T'}$ onto the right-hand side of (4.1) so we have

$$c\hat{\phi}_\zeta + [(1-\hat{\phi})\hat{v}]_\zeta = F\hat{\phi}_{T'}. \tag{4.20}$$

We now use our perturbation expansion (4.3) on (4.20) and (4.2) to find equations for $\hat{\phi}_1$ and $\hat{v}_1$. These can be written in the matrix form

$$\begin{pmatrix} \bar{p} & \bar{q} \\ \bar{r} & \bar{s} \end{pmatrix} \begin{pmatrix} \hat{\phi}_1 \\ \hat{v}_1 \end{pmatrix} = \begin{pmatrix} a_1 \\ a_2 \end{pmatrix}, \tag{4.21}$$

where the elements in the first matrix are operators and

$$a_1 = \hat{\phi}_{0T'}, \qquad a_2 = (1-\hat{\phi}_0)(\hat{v}_0 - c)\hat{v}_{0\zeta} + p_s'(\hat{\phi}_0)\hat{\phi}_{0\zeta}. \tag{4.22}$$

A solution (l_1, l_2) of the homogeneous adjoint problem to (4.21) is given in Harris & Crighton (1994) as

$$l_{1\zeta} = -\frac{\bar{r}\hat{\phi}_{0\zeta}}{(1-\hat{\phi}_0)}, \qquad l_2 = \hat{v}_{0\zeta}, \tag{4.23}$$

where

$$\bar{r} = 1 - \left(\frac{\phi_0}{\hat{\phi}_0}\right)^{n+1}\left(1 - \frac{\hat{v}_0}{\phi_0}\right)\left(1 + \frac{(n+1)(1-\hat{\phi}_0)}{\hat{\phi}_0}\right). \tag{4.24}$$

The secularity condition in integral form is then

$$\int_{-L(m,T')}^{L(m,T')} (l_1 a_1 + l_2 a_2)\, d\zeta = 0, \tag{4.25}$$

where $2L(m, T')$ is the period of the wave.

Harris & Crighton (1994) go on to show that in the infinite-wavelength case, the secularity condition (3.15) with $m = 1$ can be recovered by using suitable approximations. This also holds true for the periodic case, when $m \neq 1$, but the integration limits must be changed as well to $\pm K(m)/\kappa(T')$. Therefore no intermediate matching regions have been neglected between the weakly and fully nonlinear situations.

We now prove that the waves tend to a limiting amplitude. One half of the

secularity condition gives

$$J = -\int_{-L}^{L} l_2 a_2 \, \mathrm{d}\zeta$$
$$= 4R \int_0^L \left[c^2 \frac{(1-\phi_0)^2}{(1-\hat{\phi}_0)^2} + p_s'(\hat{\phi}_0) \right] (1-\hat{\phi}_0)^2 h(\hat{\phi}_0) \mathrm{d}\zeta. \tag{4.26}$$

The sign of J depends on the sign of the terms in square brackets in the integrand. From the definition of $p_s(\phi)$ in (2.4) and P_0 in (2.9), we have

$$p_s'(\hat{\phi}_0) = -P_0 \frac{(\phi_0 - \phi_{cp})^2}{(\hat{\phi}_0 - \phi_{cp})^2}.$$

But

$$P_0 = \alpha_0^2 - F\frac{\delta_0}{\phi_0}$$

from (2.10). Thus we need to consider the sign of

$$H(\hat{\phi}_0, c) \equiv c^2 \frac{(1-\phi_0)^2}{(1-\hat{\phi}_0)^2} - \left(\alpha_0^2 - F\frac{\delta_0}{\phi_0} \right) \frac{(\phi_0 - \phi_{cp})^2}{(\hat{\phi}_0 - \phi_{cp})^2}. \tag{4.27}$$

When $c = \alpha_0$, $\hat{\phi}_0 = \phi_0$, in the uniform state, H is positive. However, when $c = 0$, H is negative for all $\hat{\phi}_0$ as α_0 is $O(1)$ and $F \ll 1$. Thus as the wave grows and c decreases, the integral J changes sign.

The other half of the secularity condition is

$$J = \int_{-L}^{L} l_1 a_1 \, \mathrm{d}\zeta$$
$$= 2\int_0^L l_1(\hat{\phi}_0)\hat{\phi}_{0T'} \, \mathrm{d}\zeta,$$
$$= 2c_{T'} \int_0^L l_1(\hat{\phi}_0) \frac{\partial \hat{\phi}_0}{\partial c} \, \mathrm{d}\zeta, \tag{4.28}$$

as $\hat{\phi}_0 = \hat{\phi}_0(c(T'), \zeta)$. Initially, $c_{T'} < 0$ as c is decreasing so

$$I = \int_0^L l_1(\hat{\phi}_0) \frac{\partial \hat{\phi}_0}{\partial c} \, \mathrm{d}\zeta < 0 \tag{4.29}$$

as J is positive. Letting $c \to 0$, $c_{T'}$ must change sign if I remains negative. A proof that I is indeed negative as $c \to 0$ is sketched in Appendix B. Thus, there is a value of c such that $c_{T'} = 0$ and, therefore, the wave equilibrates at this velocity, with corresponding values of ϕ_l and ϕ_u.

5. Discussion

We now briefly consider the case of dilute suspensions before going on to compare our results with numerical work by Needham & Merkin (1986) and Anderson *et al.* (1995).

Firstly then, we set $\beta_0 < 0$, so

$$\phi_0 > \frac{n}{n+2}, \tag{5.1}$$

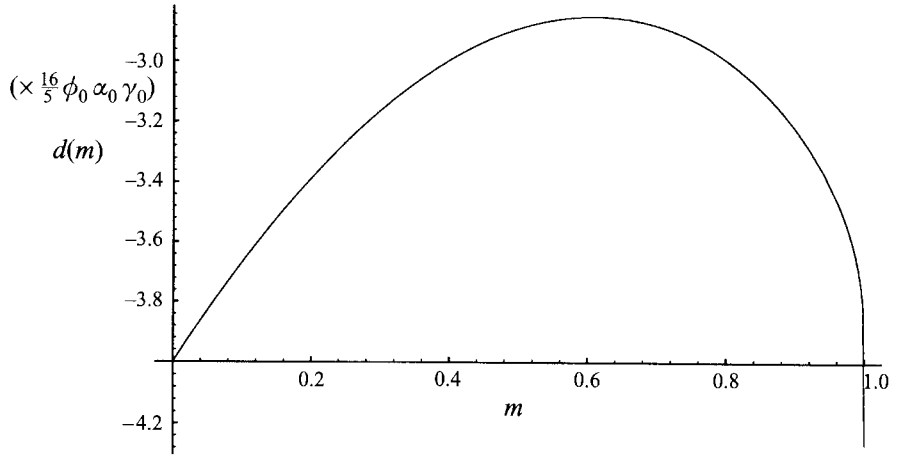

FIGURE 7. A plot of $d(m)$ for typical parameter values with $\beta_0 < 0$.

which is appropriate for hindered settling. Here, the particles in a suspension fall out under gravity, with the drag coefficient being dependent on particle concentration. Thus, if more particles are present, the drag force on each one is higher, so that the settling rate is lower than might be expected. This is essentially the same phenomenon as in fluidized beds, but in a different reference frame.

The change in sign of β_0 initially has little effect on the periodic case, but dramatically alters the situation when the infinite-wavelength soliton solution of the KdV equation is considered. Then, the soliton is inverted so that we have a more concentrated wave propagating in a dilute suspension, rather than a less concentrated, high voidage wave in a dense bed. In fact any high voidage regions in the dilute suspension will be quickly dispersed, according to standard KdV theory (see Drazin & Johnson 1989). Thus only waves of higher particle concentration can propagate.

The intial growth rate, $\kappa_T = b(m)\kappa^3$, does not depend on β_0, so this is left unaltered. However, the growth rate at larger times in (3.13) is changed since d is not independent of β_0, and a new graph of $d(m)$ in this situation is shown in figure 7. We have taken $\phi_0 = 0.7$ as a typical value, with $n = 3$ as before. Thus $d(m) < 0$ for all values of m, and so stabilization of both the cnoidal wave solutions and solitons occurs at the weakly nonlinear stage.

Needham & Merkin (1986) examine the existence of quasi-steady periodic voidage waves, using the same model equations as in this paper. The suggestion, based on results from their earlier paper Needham & Merkin (1983), is that a weakly nonlinear initial disturbance evolves and restabilizes into a quasi-periodic state. Crighton (1991) disagrees with their weakly nonlinear equation in the (1983) paper, which leads to shock discontinuties and instead derives the perturbed KdV equation. However, their suggestion of the restabilization into periodic waves is supported by our results in the previous two sections.

Needham & Merkin (1986) numerically integrate the equations, looking for travelling wave solutions. Our evolving periodic waves correspond to their subcritical case, with $c^2 < P_0$ and c decreasing giving an increasing amplitude. Their figures 4 and 5 show that the wavetrains for $\phi_0 = 0.85$ are of much smaller amplitude than those for $\phi_0 = 0.55$. This agrees with our results that for $\phi_0 > n/(n+2) \simeq 0.6$ the waves remain weakly nonlinear, whereas for $\phi_0 < n/(n+2)$ the solutions evolve to become fully

nonlinear. They also predict that waves of short wavelength are stable whereas those with longer wavelengths are unstable which is again in agreement with our results.

Anderson *et al.* (1995) numerically integrate a very similar set of equations for gas-fluidized beds, but in addition they allow the waves to evolve with time. They fix the period of the wave, which in our case would correspond to setting $K(m)/\kappa$ to be constant. Thus, we would have

$$\frac{K'(m)m_T}{K(m)} = \frac{\kappa_T}{\kappa},$$

and so m must vary on the long timescale for growing waves. This is in contrast to our choice of fixing m. Despite this, certain comparisons with our results are possible.

As an initial condition, Anderson *et al.* (1995) use a sinusoid of wavelength π cm, with a background voidage of $\phi_0 = 0.43$ and with perturbations of the order of ± 0.02. (NB Their notation is ϕ for solid fraction, which is $1 - \phi$ here.) They then track the development of this wave over time until it assumes a state which propagates unchanged. During this evolution, the wave is found to decelerate and although it grows in magnitude, it only varies by 0.03 or 0.04 from the uniform state and so satisfies a weakly nonlinear criterion.

The effect of commencing the integration with waves of longer wavelengths is qualititvely the same, but with the initial and final wave speeds being larger and the time taken to develop fully increasing. Also there is a significant increase in the highest voidages obtained and the wave now varies from -0.04 to $+0.15$ or more about the uniform state. Thus the voidage waves are much more pronounced and are fully nonlinear.

Both our results and those of Anderson *et al.* (1995) predict that small perturbations from the uniform state grow initially but those of small wavelength stabilize at a weakly nonlinear state. Longer wavelengths continue to grow, however, and become fully nonlinear. We also agree that the waves slow down as they grow, as for fixed m, c_1 becomes more negative with increasing κ from (4.18). However, for fixed κ and increasing m, c_1 becomes less negative so that the wave speeds increase with wavelength. (See figure 6.) Increasing m also has the effect of increasing T_0 in (3.10), as $b(m)$ is a decreasing function of m. This results in a longer time taken to reach the finite-time singularity when a rescaling of the equations is necessary. Therefore, a longer time is expected for the wave to obtain its final state. Thus there is very great agreement between our analytical results and the numerical results obtained by Anderson *et al.* (1995).

We note that the final state of the numerically integrated solutions for the gas-fluidized situation in Anderson *et al.* (1995) is definitely not symmetric (although the corresponding results for liquid-fluidized beds are almost symmetric). The analysis in this paper cannot predict any antisymmetry as we have only been able to find the leading-order solution and any symmetry breaking will occur at higher order (as in the soliton case in Harris & Crighton 1994). However, the numerics by Needham & Merkin (1986) only show symmetric waves, so the discrepancy could be due to the small differences in the model equations (Anderson *et al.* 1995 retain the inertia terms and have a different functional form for the particle pressure).

6. Conclusions

We began with equations for the voidage fraction ϕ and particle velocity v, which are appropriate for modelling gas-fluidized beds. Needham & Merkin (1983) showed

that the system is stable for all wavenumbers if the particle pressure P_0 is greater than the square of the linear wave speed α_0 and unstable for wavenumbers $0 < k < k_c$ for some critical k_c if $P_0 < \alpha_0^2$. Thus only the longer wavelengths grow and to examine what happens we look for a weakly nonlinear equation. The system reduces to an unstable Burgers–Korteweg–de Vries equation for the voidage, with the Froude number $F \ll 1$ as the perturbation parameter. The coefficient of the Burgers term is proportional to $P_0 - \alpha_0^2$ and so we choose this to be of $O(F)$ so that the waves are only weakly unstable. Thus our system is a perturbed KdV one, with the leading-order perturbation being an amplifying Burgers term. Amongst the $O(F^2)$ terms are some which stabilize the short wavelengths as found in the linear analysis. An extra $O(F^2)$ term omitted in Harris & Crighton (1994) is also given, although this does not affect the analysis in that paper.

We examined the temporal development of a periodic wavetrain and as our initial condition selected a cnoidal wave solution of the KdV equation. To begin with, cnoidal waves of all $O(1)$ wavelengths are amplified, with the shorter wavelengths experiencing greater growth rates. However, other terms then become important and after rescalings, it was discovered that these stabilized the shorter wavelengths in a weakly nonlinear state. The longer wavelengths continued to grow and eventually became fully nonlinear. Necessary conditions were then found for quasi-stationary fully nonlinear waves to exist. The evolution of these was investigated and they were found to match back onto the growing weakly nonlinear solutions. It was also shown that the $O(1)$ waves equilibrate so that initial finite-time singularities found in the amplitude and velocity were in fact spurious and merely a limitation due to the level of approximation.

Thus, we have analytically followed the evolution of periodic waves through from a small amplitude to final, fully nonlinear wavetrains. The results we found were in good qualitative agreement with numerical investigations by Needham & Merkin (1986) and Anderson *et al.* (1995).

The author gratefully acknowledges the support of a Darby Fellowship at Lincoln College, Oxford for the period in which this research was carried out.

Appendix A

In this Appendix, we prove a general result about integrals of even powers of the Jacobian elliptic function cn. We use the definitions given in Abramowitz & Stegun (1964), so $\mathrm{cn}\theta$ has a hidden parameter m, which can vary between 0 and 1, and a quarter-period $K(m)$.

Firstly, we consider the integral

$$I = \int_{-K}^{K} \mathrm{cn}^2\theta \frac{\mathrm{d}}{\mathrm{d}\theta}(\mathrm{cn}^{2n-1}\theta\,\mathrm{sn}\theta\,\mathrm{dn}\theta)\,\mathrm{d}\theta, \tag{A 1}$$

and integrate by parts to yield

$$I = \int_{-K}^{K} 2\mathrm{cn}^{2n}\theta\,\mathrm{sn}^2\theta\,\mathrm{dn}^2\theta\,\mathrm{d}\theta, \tag{A 2}$$

as $\mathrm{cn}(\pm K) = 0$. But we also note that the other Jacobian elliptic functions are related to $\mathrm{cn}\theta$ by

$$\mathrm{sn}^2\theta = 1 - \mathrm{cn}^2\theta, \qquad \mathrm{dn}^2\theta = 1 - m + m\mathrm{cn}^2\theta, \tag{A 3}$$

so that

$$I = 2\int_{-K}^{K} \mathrm{cn}^{2n}\theta[1 - m + (2m-1)\mathrm{cn}^2\theta - m\mathrm{cn}^4\theta]\,\mathrm{d}\theta. \tag{A 4}$$

However, if we differentiate the $\mathrm{cn}^{2n-1}\theta\,\mathrm{sn}\theta\,\mathrm{dn}\theta$ term in (A 1) and use the identities in (A 3), we also obtain

$$I = \int_{-K}^{K} 2\mathrm{cn}^{2n}\theta[(2n+1)m\mathrm{cn}^4\theta + 2n(1-2m)\mathrm{cn}^2\theta + (2n-1)(m-1)]\,\mathrm{d}\theta. \tag{A 5}$$

Therefore equating (A 4) and (A 5), we obtain the identity

$$\int_{-K}^{K} \mathrm{cn}^{2n}\theta[(2n+3)m\mathrm{cn}^4\theta + (2n+2)(1-2m)\mathrm{cn}^2\theta + (2n+1)(m-1)]\,\mathrm{d}\theta = 0, \tag{A 6}$$

and this holds for all m and for all $n \geqslant 0$.

Appendix B

Here, we sketch a proof to show that

$$I = \int_0^L l_1(\hat{\phi}_0)\hat{\phi}_{0\zeta}\,\mathrm{d}\zeta \tag{B 1}$$

is negative as $c \to 0$. In the analysis which follows we drop the hat and the zero subscript on $\hat{\phi}_0$ for simplicity.

Firstly, we examine the function $l_1(\phi)$. This is defined in (4.23) by

$$l_{1\zeta} = -\frac{\bar{r}\phi_\zeta}{(1-\phi)}, \tag{B 2}$$

with

$$\bar{r} = 1 - \left(\frac{\phi_0}{\phi}\right)^{n+1}\left(1 + \frac{c}{\phi_0}\frac{(\phi-\phi_0)}{(1-\phi)}\right)\left(1 + \frac{(n+1)(1-\phi)}{\phi}\right), \tag{B 3}$$

from (4.24) and (4.4). Thus

$$l_{1\zeta} = \left[h'(\phi) + \left(\frac{\phi_0}{\phi}\right)^{n+1}\left(1 + \frac{c}{\phi_0}\frac{(\phi-\phi_0)}{(1-\phi)}\right)\frac{(n+1)}{\phi}\right]\phi_\zeta, \tag{B 4}$$

using the definition of $h(\phi)$ in (4.6). Integrating this expression and requiring $l_1(\phi_0) = 0$ for matching back to the weakly nonlinear scenario gives

$$l_1(\phi,c) = h(\phi,c) - h(\phi_0,c) + 1 - \left(\frac{\phi_0}{\phi}\right)^{n+1} + \frac{c}{\phi_0}\int_{\phi_0}^{\phi}\left(\frac{\phi_0}{z}\right)^{n+1}\frac{(n+1)(z-\phi_0)}{z(1-z)}\,\mathrm{d}z, \tag{B 5}$$

where we have now made explicit the dependence of l_1 and h on c. Setting $c = 0$, we have

$$l_1(\phi,0) = h(\phi,0) - h(\phi_0,0) + 1 - \left(\frac{\phi_0}{\phi}\right)^{n+1}. \tag{B 6}$$

A graph of $l_1(\phi,0)$ is shown in figure 8, with $n = 3$ and $\phi_0 = 0.4$. It can be seen that $l_1(\phi,0) < 0$ for $\phi < \phi_0$ and is positive for $\phi > \phi_0$ unless ϕ is close to 1. But, we note that $h'(\phi)$ is positive for $\phi < \phi_0$ and negative for $\phi > \phi_0$, with $h(\phi_l) = h(\phi_u) = 0$. Therefore integrating (4.6) taking ϕ_l to be 0.27, the smallest possible value for which

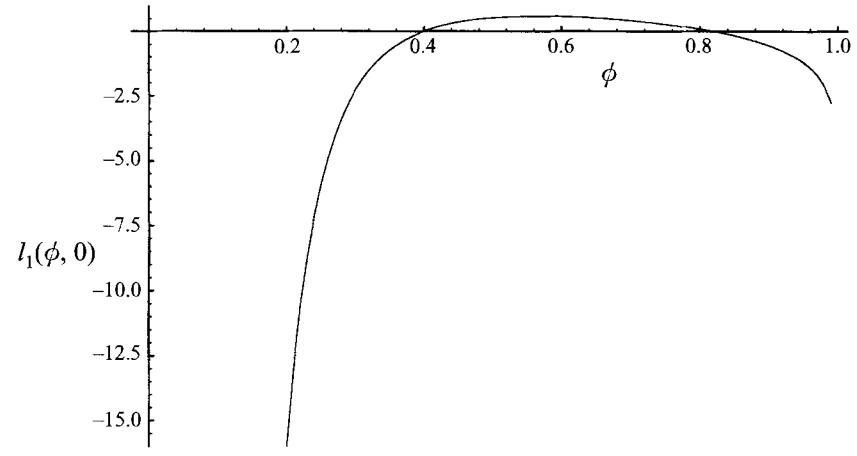

FIGURE 8. The function $l_1(\phi,0)$ plotted against ϕ.

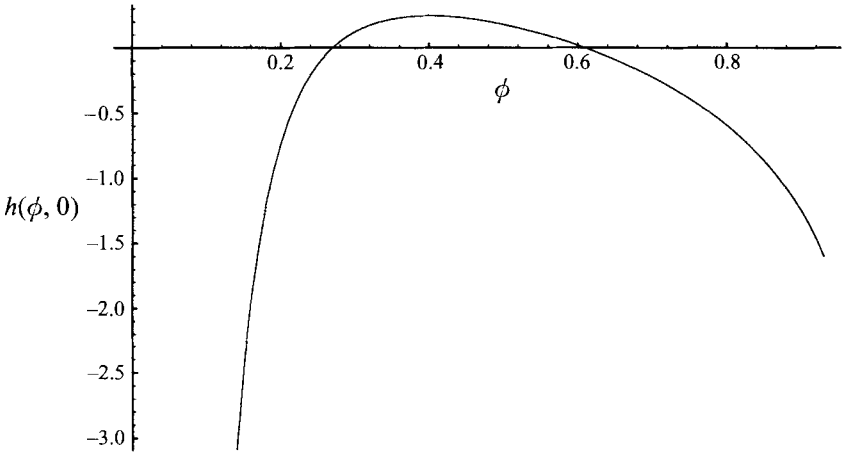

FIGURE 9. A graph of $h(\phi,0)$ with the smallest zero of h taken to be $\phi_l = 0.27$.

the bed is fluidized, gives the largest value of ϕ_u. From figure 9, this shows that the maximum ϕ_u is approximately 0.6. Thus $l_1(\phi,0) > 0$ in the range $\phi_0 < \phi < \phi_u$.

To find ϕ_c, we start by writing (4.5) in the form

$$\phi_\zeta{}^2 = \frac{2R}{c(1-\phi_0)}(1-\phi)^4 h(\phi,c). \tag{B 7}$$

Now differentiating with respect to c and rearranging gives

$$\phi_{\zeta c} + \frac{R(1-\phi)^3}{c(1-\phi_0)}[4h(\phi,c) - (1-\phi)h'(\phi,c)]\frac{\phi_c}{\phi_\zeta} = \frac{R(1-\phi)^4}{c^2(1-\phi_0)\phi_\zeta}\left[c\frac{\partial h}{\partial c}(\phi,c) - h(\phi,c)\right], \tag{B 8}$$

where $'$ denotes a ϕ-derivative. The equation

$$\frac{\mathrm{d}}{\mathrm{d}\zeta}[w(\phi)\phi_c] = y(\phi) \tag{B 9}$$

results in

$$\phi_{\zeta c} + \frac{w'(\phi)}{w(\phi)}\phi_\zeta \phi_c = \frac{y(\phi)}{w(\phi)}. \tag{B 10}$$

Comparing this with (B 8) gives

$$\frac{w'(\phi)}{w(\phi)} = \frac{2}{(1-\phi)} - \frac{h'(\phi)}{2h(\phi)}, \tag{B 11}$$

on using (B 7) to replace ϕ_ζ^2. Therefore, we have

$$w(\phi) = w(\phi_0)\left(\frac{1-\phi_0}{1-\phi}\right)^2 \left(\frac{h(\phi_0)}{h(\phi)}\right)^{1/2}. \tag{B 12}$$

We also find from (B 8) that

$$y(\phi) = -\frac{R(1-\phi)^4}{c^2(1-\phi_0)} h(\phi, 0)\frac{w(\phi)}{\phi_\zeta}, \tag{B 13}$$

as

$$h(\phi, c) - c\frac{\partial h}{\partial c} = h(\phi, 0),$$

from the definition of h in (4.6). Thus integrating (B 9) yields

$$\phi_c = \frac{-1}{2cw(\phi)} \int_{\phi_0}^{\phi} \frac{h(\phi, 0)}{h(\phi, c)} w(\phi)\, \mathrm{d}\phi \tag{B 14}$$

and letting $c \to 0$, we have

$$\phi_c \sim \frac{-1}{2c}\phi_\zeta(\zeta - \zeta_0), \tag{B 15}$$

where ζ_0 is such that $\phi(\zeta_0) = \phi_0$. We note that for ζ in $[0, L]$, $\phi_\zeta < 0$, so that for $\zeta < \zeta_0$, i.e. $\phi > \phi_0$, we have $\phi_c < 0$, whereas for $\zeta > \zeta_0$, i.e. $\phi < \phi_0$, then $\phi_c > 0$. Combining this with the signs of $l_1(\phi, 0)$ in the relevant ranges shows that

$$\int_0^L l_1(\phi)\phi_c \, \mathrm{d}\zeta < 0, \tag{B 16}$$

as $c \to 0$.

REFERENCES

Abramowitz, M. & Stegun, I. A. 1964 *Handbook of Mathematical Functions.* National Bureau of Standards.

Anderson, K., Sundaresan, S. & Jackson, R. 1995 Instabilities and the formation of bubbles in fluidized beds. *J. Fluid Mech.* **303**, 327–366.

Courant, R. & Hilbert, D. 1962 *Methods of Mathematical Physics*, Vol II. Wiley–Interscience.

Crighton, D. G. 1991 Nonlinear waves in fluidized beds. In *Nonlinear Waves in Real Fluids* (ed. A. Kluwick), pp. 83–90. Springer.

Crighton, D. G. 1995 Applications of KdV. *Acta Appl. Math.* **39**, 39–67.

Drazin, P. G. & Johnson, R. S. 1989 *Solitons: an Introduction.* Cambridge University Press.

Foscolo, P. U. & Gibilaro, L. G. 1984 A fully predictive criterion for the transition between particulate and aggregate fluidization. *Chem. Engng Sci.* **39**, 1667–1675.

Foscolo, P. U. & Gibilaro, L. G. 1987 Fluid dynamic stability of fluidized suspensions: the particle bed model. *Chem. Engng Sci.* **42**, 1489–1500.

Garg, S. K. & Pritchett, J. W. 1975 Dynamics of gas–fluidized beds. *J. Appl. Phys.* **46**, 4493–4500.

Göz, M. F. 1993 Bifurcations of plane voidage waves in fluidized beds. *Physica* D **65**, 319–351.

HARRIS, S. E. & CRIGHTON, D. G. 1994 Solitons, solitary waves and voidage disturbances in gas-fluidized beds. *J. Fluid Mech.* **266**, 243–276.

HOMSY, G. M., EL-KAISSY, M. M. & DIDWANIA, A. 1980 Instability waves and the origin of bubbles in fluidized beds. Part II. *Intl J. Multiphase Flow* **6**, 305–318.

JACKSON, R. 1963*a* The mechanics of fluidised beds. Part I. The stability of the state of uniform fluidisation. *Trans. Instn Chem. Engrs* **41**, 13–21.

JACKSON, R. 1963*b* The mechanics of fluidised beds. Part II. The motion of fully developed bubbles. *Trans. Instn Chem. Engrs* **41**, 22–28.

LEIBOVICH, S. & SEEBASS, A. R. 1974 *Nonlinear Waves.* Cornell University Press.

LEVA, M. 1959 *Fluidization.* McGraw-Hill.

MURRAY, J. D. 1965 On the mathematics of fluidization. *J. Fluid Mech.* **21**, 465–493.

NAYFEH, A. H. 1973 *Perturbation Methods.* Wiley–Interscience.

NEEDHAM, D. J. & MERKIN, J. H. 1983 The propagation of a voidage disturbance in a uniformly fluidized bed. *J. Fluid Mech.* **131**, 427–454.

NEEDHAM, D. J. & MERKIN, J. H. 1986 The existence and stability of quasi–steady periodic voidage waves in a fluidized bed. *Z. Angew. Math. Phys.* **37**, 322–339.

RICHARDSON, J. F. 1971 Incipient fluidization and particulate systems. In *Fluidization* (ed. J.F. Davidson & D. Harrison), pp. 26–64. Academic.